Journal of Alloys and Compounds 512 (2012) 235–240

Contents lists available at SciVerse ScienceDirect

Journal of Alloys and Compounds

journal homepage: www.elsevier.com/locate/jallcom

Dual codoping for the fabrication of low resistive *p*-ZnO

L. Balakrishnan[a], S. Gowrishankar[a], P. Premchander[b], N. Gopalakrishnan[a,*]

[a] Thin Film Laboratory, Department of Physics, National Institute of Technology, Tiruchirappalli 620015, India
[b] Centre for Information Technology Education, Department of Information & Communications, Gwangju Institute of Science and Technology, Gwangju 500-712, South Korea

ARTICLE INFO

Article history:
Received 16 November 2010
Received in revised form 25 July 2011
Accepted 21 September 2011
Available online 29 September 2011

Keywords:
ZnO
Dual codoping
Sputtering
Characterization

ABSTRACT

A dual codoping method has been proposed to fabricate low resistive and stable *p*-ZnO thin films. Both nitrogen (N) and arsenic (As) have been used as acceptors while aluminum (Al) as donor in our dual codoping process. The As–Al–N dual codoped ZnO films have been prepared by RF magnetron sputtering on GaAs substrate using AlN doped ZnO targets (0.5, 1 and 2 mol%). In our dual codoping approach, Al and N from target and As from GaAs substrate (back diffusion) take part. X-ray diffraction (XRD), room temperature and low temperature photoluminescence (PL), electron probe micro analysis (EPMA), energy dispersive spectroscopy (EDS), atomic force microscopy (AFM) and Hall effect measurement have been performed to investigate the effect of AlN concentration on the dual codoped ZnO films. All the films (0, 0.5 and 1 mol%) showed *p*-type conductivity except 2 mol% AlN doped film. The lowest room temperature resistivity, $8.6 \times 10^{-2}\ \Omega$ cm has been achieved with a hole concentration of the order, 10^{20} cm^{-3} for the optimum 1 mol% AlN concentration. The observed resistivity is much lower than that of monodoped (As or N) and codoped (AlN or AlAs) ZnO films. The *p*-type conductivity has been explained by the new complex formation mechanism.

1. Introduction

The higher excitonic binding energy (60 meV) of ZnO makes it as a prime candidate than the group III nitrides for the fabrication of UV-LEDs and lasers [1,2]. To date, some of these devices have been realised and others are under progress. In general, the critical point for wide band gap materials is to achieve low resistivity and high carrier concentration which are necessary for device functionality. The efficiency of the ZnO based optoelectronic devices strongly depends on the electrical and optical properties of both *n* and *p*-type ZnO films. Due to the native defects of ZnO, it is easy to grow low resistive *n*-ZnO with good optical properties even without any intentional doping [3,4]. However, for light emitters, stable *p*-ZnO with high hole concentration and low resistivity is required. This remains the major bottleneck for ZnO based optoelectronic devices with high efficiency.

According to the density functional theory, the *cationic* substitution of group I elements such as Li, Na and K for *p*-conductivity leads to several drawbacks (high diffusivity and self compensation effect) [5]. Also, the *anionic* substitution of group V elements, such as N, P and As forms deep acceptor level instead of shallow level [5]. Hence, the concept, codoping (simultaneous doping of *one* acceptor and *one* donor) has been proposed instead of monodoping. In codoping more acceptors are facilitated due to the formation of acceptor–donor–acceptor complexes [6–9].

Following Wang and Zunger [10], we present here a different approach, called dual codoping (triple doping or cluster doping), i.e. simultaneous doping of *two* acceptors (arsenic and nitrogen) and *one* donor (aluminum) into ZnO to realise *p*-conductivity. Among the *p*-type dopants, N and As have been considered as the best acceptors since N has similar atomic radius as that of O, it leads to the formation of a shallow acceptor level compared to the other group V elements. Similarly, As substitution on Zn site leads to the formation of a shallow acceptor (As_{Zn}–$2V_{Zn}$) [11]. Aluminum has been used as a donor because it has similar atomic radius as that of Zn. It also improves the crystalline quality of the film [12,13].

Here, we demonstrated that dual codoping is a promising method to produce low resistivity and stable *p*-ZnO thin films with high hole concentration.

2. Experimental

Monodoped (As) and dual codoped (As–Al–N) ZnO thin films have been prepared on GaAs (1 0 0) substrate by RF magnetron sputtering. In our dual codoping process, GaAs substrate itself acting as a source of supplying As atoms while AlN mixed ZnO target acts as a source of Al and N atoms. Arsenic atoms can back-diffuse from the GaAs substrate into ZnO lattice by supplying thermal energy to the substrate. The different concentrations (0.5, 1 and 2 mol%) of AlN doped ZnO targets have been prepared by conventional solid state reaction route which has been explained as follows. The required amount of AlN powder (99.99% purity) has been mixed uniformly with the host ZnO (99.99% purity) using ball mill for 10 h. The mixture has been made into a circular disc using hydraulic press. The circular disc has been

* Corresponding author. Tel.: +91 431 2503607; fax: +91 431 2500133.
E-mail address: ngk@nitt.edu (N. Gopalakrishnan).

0925-8388/$ – see front matter © 2011 Elsevier B.V. All rights reserved.
doi:10.1016/j.jallcom.2011.09.072

Table 1
Hall effect measurement results of monodoped and dual codoped ZnO films with different AlN doping concentration.

AlN concentration (mol%)	Carrier type	Carrier concentration (cm^{-3})	Resistivity (Ω cm)	Mobility (cm^2/V s)
0	p	9.33×10^{15}	18.67	35.82
0.5	p	5.03×10^{19}	3.86×10^{-2}	3.602
1	p	4.72×10^{20}	8.63×10^{-2}	0.536
2	n	1.17×10^{20}	8.35×10^{-2}	0.867

densified by sintering at 950 °C for 6 h. Similarly, pure ZnO target has also been prepared for monodoping. Thus prepared targets have been used for the film growth.

Before the film deposition, the substrate has been cleaned with boiling acetone and then rinsed in ethanol followed by distilled water. The process has been repeated for five times to remove the surface contaminations and then finally blown with dry air. The substrate has been fixed at a distance of 5 cm from the target. Initially, the sputtering chamber has been evacuated to a base pressure of 8×10^{-6} mbar. The ($Ar + O_2$) pressure of 0.02 mbar has been used for the film growth. The films have been grown at a substrate temperature, 450 °C for 30 min with the RF power of 100 W. Prior to the film deposition, pre-sputtering has been carried out to remove the surface contaminations on the target. The thickness of the films measured by Filmetrics (F20) has been found as ~110 nm.

As mentioned earlier, As from the GaAs substrate and Al & N from the target take part in our dual codoping process. The substrate temperature, 450 °C has been used to avoid the incorporation of Ga atoms into ZnO as the vapour pressure of Ga is much lower than that of As below 500 °C [14]. The electrical properties of the films have been studied by Hall measurements in Van der Pauw configuration (HMS 3000) at room temperature. Indium electrodes have been made on the four corners of the films. Prior to the measurement, the ohmic behaviour between indium electrodes has been confirmed. The crystalline quality of the films has been analysed by XRD with a wavelength of 1.5406 Å (Cu Kα). The Xenon lamp and He–Cd laser (wavelength, 325 nm) have been used as the excitation sources for room temperature and low temperature PL measurements, respectively. The elemental analyses of the films have been done by EPMA and EDS.

3. Characterization

3.1. Electrical properties

The electrical properties of the films have been measured by Van der Pauw–Hall effect measurement and the results are illustrated in Table 1. It is well known that substitutional Zn on O site (Zn_O), Zn interstitial (Zn_i), O vacancies (V_O), As interstitial (As_i), As on Zn antisite (As_{Zn}) and N interstitial (N_i) are donors, while Zn vacancy (V_{Zn}), O interstitial (O_i), As on O site (As_O) and N on O site (N_O) are acceptors [15,16]. Hence, the *p*-conductivity of the films may ascribe to the following factors; formation of (i) acceptors such as N_O and As_O induced by the dopants and (ii) V_{Zn} due to the formation of As_{Zn}–$2V_{Zn}$ complex.

The monodoped ZnO shows *p*-conductivity with the carrier concentration of the order of 10^{15} cm^{-3}. It is due to the incorporation of As atoms on Zn site that leads to the formation of As_{Zn}–$2V_{Zn}$ acceptor complex instead of As_O because of its high formation energy [11]. However, in the case of 0.5 and 1 mol% AlN doped ZnO, the hole concentration increases to the order of 10^{19} and 10^{20} cm^{-3}, respectively. This is due to the incorporation of N atoms on O site (N_O) and As on Zn site. The reason is that the probability of As to sit on O site (As_O) is low compared with N (N_O) due to the higher acceptor ionization energy of As_O (~930 meV). Among these two films, 1 mol% AlN doped ZnO showed low resistivity (8.6×10^{-2} Ω cm) with high hole concentration. This is much better than monodoped [17,18] and codoped [19] films. Further, the *p*-conductivity of the films has been found as stable even after 6 months. In the case of 2 mol% AlN doped ZnO:As, the conductivity changes from *p*- to *n*-type. This change or disappearance of *p*-type behaviour is due to the more incorporation of Al and N atoms which lead to the dissociation of Al_{Zn}–$2N_O$ and As_{Zn}–$2V_{Zn}$ acceptor complexes into various donor complexes such as Al_{Zn}, Zn_i, $(N_2)_O$, N_i, As_{Zn}, As_{Zn}–V_{Zn}, etc. [15,16]. Hence, optimum AlN concentration is necessary to obtain *p*-ZnO.

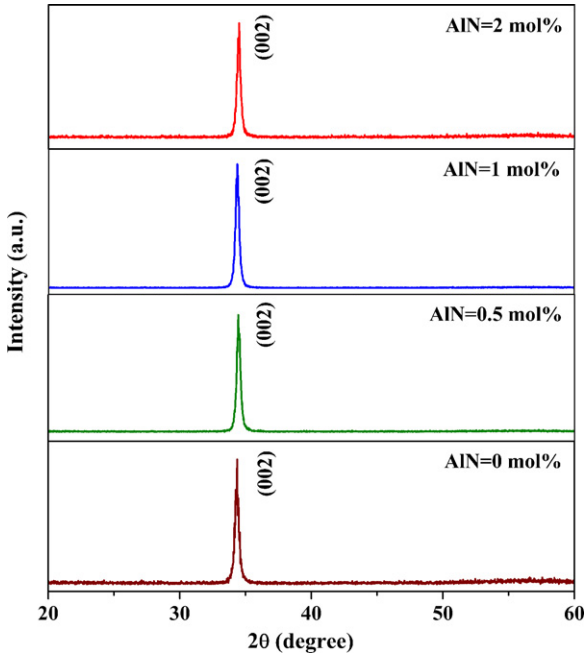

Fig. 1. XRD pattern of monodoped and dual codoped ZnO films.

3.2. Structural properties

Fig. 1 shows the XRD pattern of monodoped and dual codoped ZnO films. It is seen that all the films are in (0 0 2) preferential orientation and no other diffraction peaks correspond to secondary phases have been observed. King et al. reported that the position of (0 0 2) peak has been related to the film stoichiometry and lattice imperfections [20]. The *c*-axis lattice constant corresponds to (0 0 2) peak position has been calculated using the Bragg's relation, $c = \lambda/\sin\theta$, where λ is the wavelength of the X-ray used and θ is the position of the (0 0 2) peak.

The variation of *c*-axis lattice constant for monodoped and dual codoped ZnO films as a function of AlN concentration is shown in Fig. 2. In the case of monodoped film, the incorporation of As increase *c*-axis lattice constant and hence causes tensile strain in the film [21]. In dual codoped film, N, As and Al have been incorporated into ZnO lattice. According to first principle calculation, the ionization energy of N_O is very low compared to the ionization energy of As_O [22]. This leads to the formation of more N_O compared to As_O. Hence, the incorporation of more N atoms on O site causes the incorporation of As atoms on Zn site. In the case of 0.5 mol% AlN doped ZnO, the compressive stress is due to the incorporation of smaller ionic radius Al and As on Zn site. The tensile strain for 1 mol% AlN doped ZnO is due to the more incorporation of higher ionic radius N atoms on O site. This has been reported as a best codoping concentration due to the incorporation of more N atoms in our previous work [23]. For 2 mol% ZnO, though it is compressive stress, the more incorporation of smaller ionic radius Al atoms on Zn site results in *n*-conduction as seen in our Hall effect measurement.

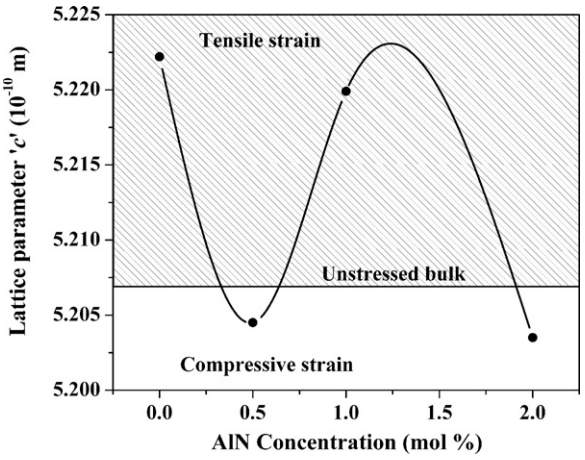

Fig. 2. Variation of *c*-axis lattice as a function of AlN concentration.

3.3. Elemental analysis

3.3.1. Electron probe microanalysis and energy dispersive spectroscopy

The EPMA analysis has been performed in order to confirm the presence of arsenic in the film which has been diffused from the substrate. Fig. 3 shows the EPMA spectrum of the film grown from 1 mol% AlN doped ZnO target on GaAs substrate. In order to make ionization only in the film (i.e. to reduce the depth of ionization), low energy electrons (acceleration potential—5 kV) have been used for the analysis. The concentration of Zn, Al and As has been determined as 84.3, 0.8 and 14.9 at%, respectively. It should be noted that the presence of Ga has not been observed which indicates that only As atoms have been diffused into the film from the substrate.

Due to overlap of the peaks, O and N have not been detected in the EPMA analysis. Hence, EDS analysis has been performed to confirm the presence of N and O in the film. EDS spectrum has been recorded at an electron acceleration potential of 10 kV. Fig. 4 shows the EDS spectra with elemental composition of 1 mol% AlN doped ZnO:As film. It should be noted that N and O have been observed with other elements.

It is worthy to note that there is a fair difference in the composition of the elements observed in both methods because EDS analysis has been performed (using high energy electrons) relatively deeper than EPMA (using low energy electrons) in the film. It is obvious that in diffusion method, the concentration of the diffused atoms (As) is high at the substrate–film interface and gradually decreases till the film surface. This result in high concentration of As atoms measured from EDS analysis than EPMA which in turn alters the composition of the other elements.

3.4. Theoretical mechanism

The mechanism of the dual codoping is more complex. However, we proposed a possible mechanism based on the theoretical

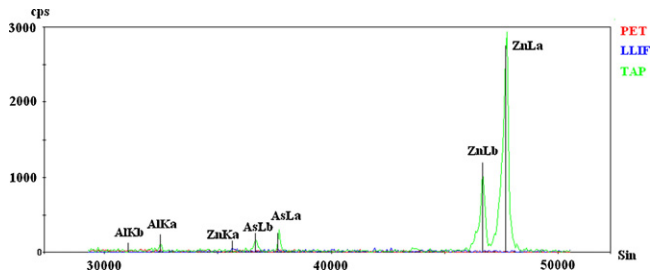

Fig. 3. EPMA spectrum of 1 mol% AlN doped ZnO:As film.

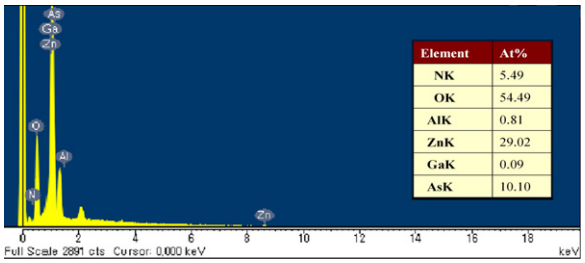

Fig. 4. EDS spectra of 1 mol% AlN doped ZnO film on GaAs substrate.

analysis. In the case of As doped ZnO (monodoping), the large size mismatch between As and O inhibits the substitution of As on O site [11]. Indeed, first-principle calculation [11] shows that large size mismatched group V elements (except N) prefer to substitute on Zn rather than O because high ionization energy is required for O substitution. Based on this, here we suggested that As prefers to sit on Zn antisite (As_{Zn}) and subsequently induces two zinc vacancies (V_{Zn}) to form As_{Zn}–$2V_{Zn}$ complex. In this complex, As atom is a *triple donor* while zinc vacancy is a *double acceptor* and hence the As atom donates all of its three electrons to the two zinc vacancies. Since, there is shortage of one electron which creates a hole [24]. Thus, the formation of a hole can be explained as follows:

$$As_{Zn}^{3+} + V_{Zn}^{2-} \rightarrow (As_{Zn}–V_{Zn})^{+} + V_{Zn}^{2-} \rightarrow (As_{Zn}–2V_{Zn})^{-}$$

The resulting (As_{Zn}–$2V_{Zn}$) complex forms shallow acceptor level with a hole ionization energy of ~200 meV [11]. There have been several reports that As_{Zn}–$2V_{Zn}$ complex is the most possible acceptor in As doped ZnO films [24–26].

Similarly, in the case of AlN doped ZnO (codoping), Al sits on Zn site (Al_{Zn}) and N sits on O site. Due to the formation of N–Al–N complex, Al facilitates more N atoms [27]. This can be explained as follows:

$$Al_{Zn}^{3+} + N_{O}^{3-} + N_{O}^{3-} \rightarrow (Al_{Zn}–2N_{O})^{-}$$

The resulting complex as well forms shallow acceptor level with a hole ionization energy of ~170 meV [28].

In our dual *codoping, we have used these two advantages to realise low resistive p*-ZnO. Also, the more incorporation of N is beneficial for the formation of As_{Zn} rather than As_{O}. Hence the formation of the new complex in dual codoping has been given below:

$$(As_{Zn}–2V_{Zn})^{-} + (Al_{Zn}–2N_{O})^{-} \rightarrow (Al_{Zn} + As_{Zn}–2V_{Zn}–2N_{O})^{2-}$$

The low ionization energy for N on O substitution causes As to sit on Zn site. This leads to the formation of As_{Zn}–$2V_{Zn}$ complex which is also responsible for *p*-conduction in addition to N_{O}. Hence, we proposed that the new complex (Al_{Zn} + As_{Zn}–$2V_{Zn}$–$2N_{O}$) formed in our dual codoping process which is responsible for the *p*-conduction.

3.5. Optical properties

3.5.1. Room temperature photoluminescence

In order to investigate the optical properties, the grown films have been subjected to PL analysis. Fig. 5 shows the room temperature PL spectra of the monodoped and dual codoped ZnO films of different AlN concentrations. All the films exhibit a predominant NBE emission at around 3 eV accompanying with low intensity deep level emissions (DLE) in the range 2.1–2.8 eV. This indicates that all the films exhibit high optical quality. The blue band (BB) emission at around 2.8 eV is due to the lattice distortion induced by the incorporation of size mismatched atoms such as As and N [29]. The green band (GB) emission at around 2.5 eV results from the radial recombination of a photo generated hole with an electron [30]. The yellow

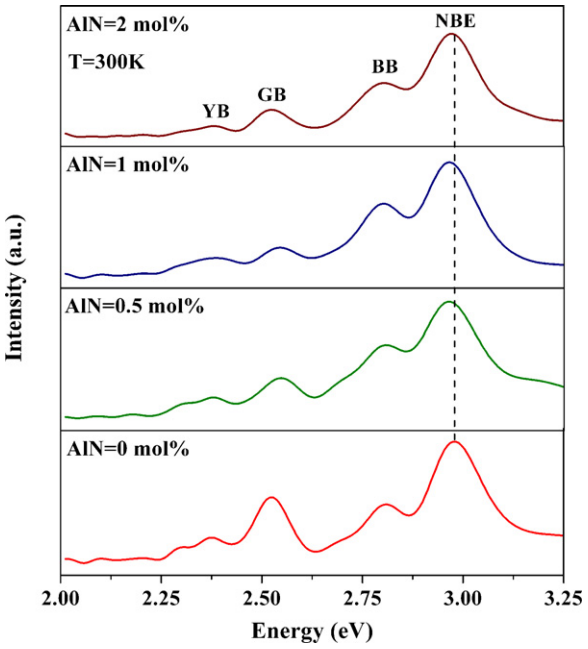

Fig. 5. Room temperature PL spectra of monodoped and dual codoped ZnO films of different AlN concentration.

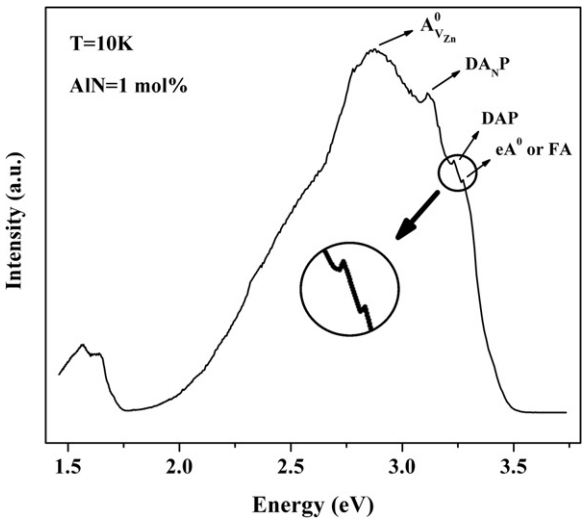

Fig. 6. Low temperature PL spectra of 1 mol% AlN doped ZnO on GaAs substrate.

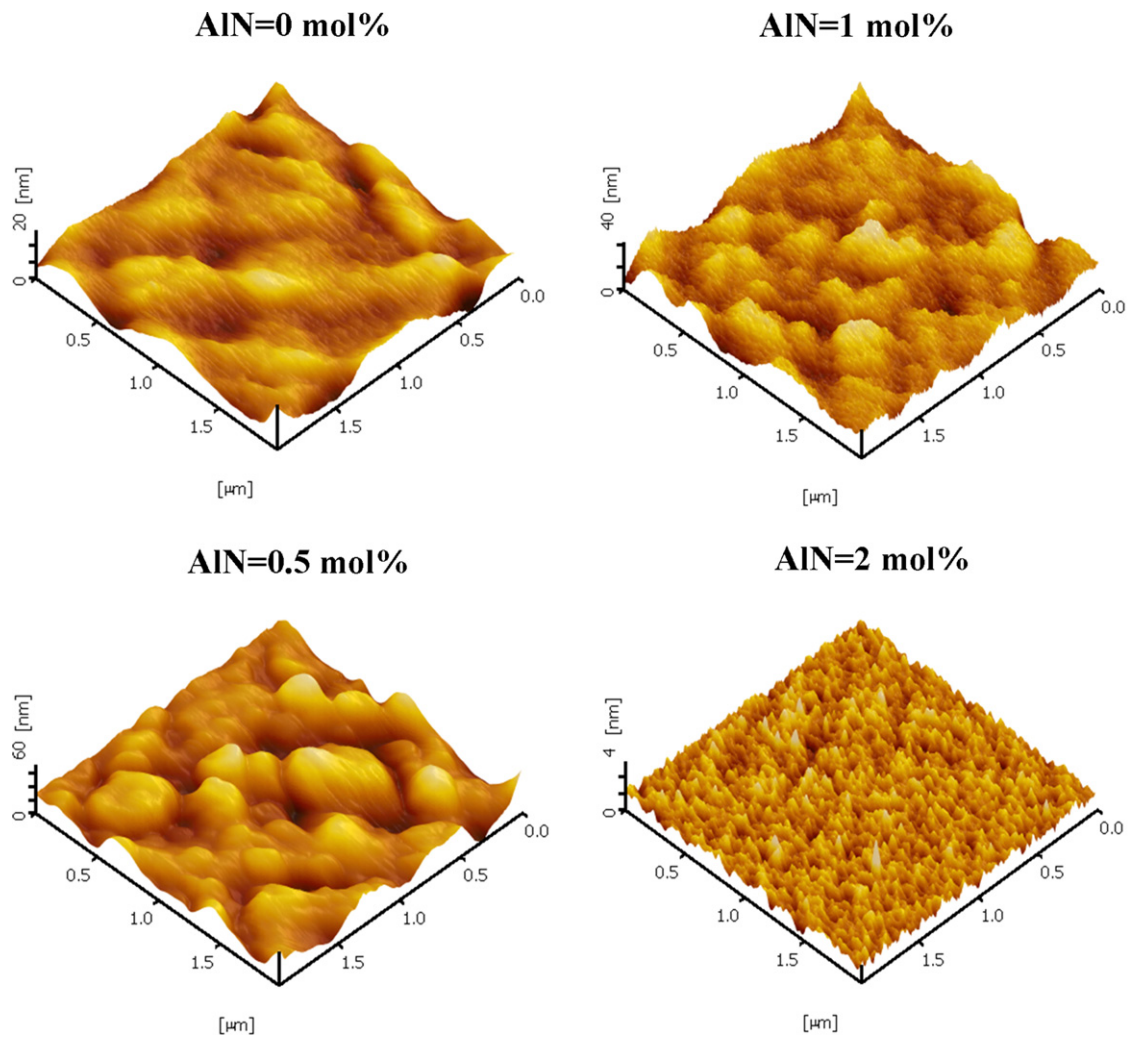

Fig. 7. AFM images of monodoped and dual codoped ZnO films of different AlN concentration.

band (YB) emission at around 2.4 eV is due to the recombination of free electrons and deep acceptor defects (i.e. O_i) [31,32]. The red shift in NBE indicates the increase in hole concentration for dual codoped films compared to the monodoped film [33]. The increase in intensity of blue band emission for 0.5 and 1 mol% AlN doping concentrations also acknowledges the more incorporation of N and As ions into the ZnO lattice. This has been well supported by our XRD and Hall results.

3.5.2. Low temperature photoluminescence

In order to understand the origin of *p*-type conductivity of the dual codoped ZnO films in better manner, low temperature (10 K) PL measurement has been performed. Fig. 6 shows the low temperature PL spectrum of 1 mol% AlN doped ZnO:As film. The dominant emission peak located at around 2.9 eV is attributed to the transition of excited electron to V_{Zn} acceptor level [34,35]. This emission has been ascribed to the substitution of As on Zn site $\left(As^{O}_{V_{Zn}}\right)$. Similar dominant emission peak has also been observed by Rogers et al. for the As back diffused *p*-ZnO film grown on GaAs substrate [36]. The peak located at 3.12 eV is related to the donor–acceptor pair involving N acceptors (DA_NP), i.e. due to the substitution of N on O site (N_O) [37]. The peak at 3.23 eV is ascribed to the donor–acceptor pair (DAP) transition which confirms the presence of acceptors in the film [38,39]. Another peak located at 3.27 eV is attributed to the free exciton to neutral-acceptor (eA^0) recombination [40] or free electron-acceptor (FA) recombination [41] which confirms the *p*-conductivity of the films. Hence, it can be concluded that the *p*-conductivity has been originated due to both (As_{Zn}–$2V_{Zn}$) and (Al_{Zn}–$2N_O$) complexes. The domination of peak corresponds to V_{Zn} compared to N_O implies that the *p*-type conduction has been mainly from the contribution of holes supplied by the As atoms diffused from the GaAs substrate.

3.6. Morphological analysis

The surface morphology of both monodoped and dual codoped ZnO films have been investigated by AFM (Fig. 7). Among the roughness parameters, peak to valley roughness (R_{PV}) is important one for the optoelectronic device functionality, i.e. the leakage current increases with the increase of R_{PV} [42]. Fig. 8 shows the variation of R_{PV} as a function of AlN concentration. Since 1 mol% AlN doped ZnO has low R_{PV} with high hole concentration and low resistivity, it is more suitable for device applications. Hence, it can be concluded that 1 mol% AlN doped ZnO is a best dual codoped film in the chosen experimental parameters.

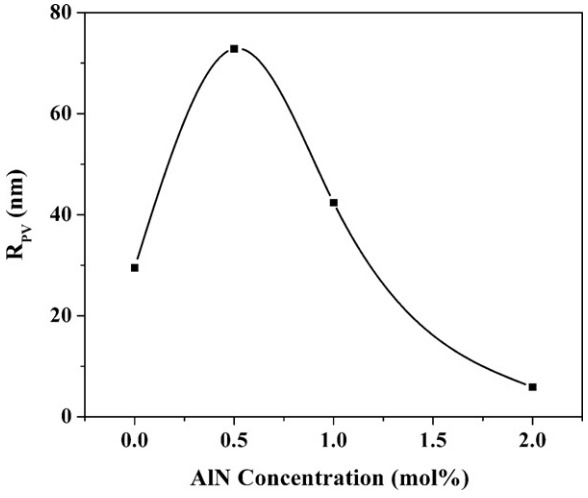

Fig. 8. Variation of R_{PV} as a function of AlN concentration.

4. Conclusion

In summary, the As–Al–N dual codoped ZnO films have been grown on GaAs substrate by RF magnetron sputtering using AlN doped ZnO targets. The back-diffusion of As atoms from the GaAs substrate upon supplying the thermal energy has been used as the As source. The grown films have been evaluated by XRD, room temperature and low temperature PL, Hall effect, EPMA, EDS and AFM. In the optimised experimental conditions, 1 mol% AlN dual codoped ZnO:As film exhibited strong *p*-conductivity (4.72×10^{20} cm^{-3}) with low resistivity (8.6×10^{-2} Ω cm) compared to monodoped and codoped films. This has been explained by the new complex ($Al_{Zn} + As_{Zn}$–$2V_{Zn}$–$2N_O$) formation mechanism. It is suggested that the dual codoping is the promising approach for the fabrication of low resistive *p*-ZnO to realise practical devices.

References

[1] S.J. Pearton, D.P. Norton, K. Ip, Y.W. Heo, T. Steiner, J. Vac. Sci. Technol. B 22 (2004) 932.
[2] D.C. Look, B. Claflin, Phys. Status Solidi B 241 (2004) 624.
[3] P. Zhu, Z.K. Tang, G.K.L. Wong, M. Kawasakii, A. Ohtomo, H. Koinuma, Y. Segawa, Solid State Commun. 103 (1999) 459.
[4] J.G. Lu, Z.Z. Ye, Y.J. Zeng, L.P. Zhu, L. Wang, J. Yuan, B.H. Zhao, Q.L. Liang, J. Appl. Phys. 100 (2006) 073714.
[5] C.H. Park, S.B. Zhang, S.H. Wei, Phys. Rev. B 66 (2002) 073202.
[6] T. Yamamoto, H.K. Yoshida, Jpn. J. Appl. Phys. Part 2 38 (1999) L166.
[7] J.G. Lu, Z.Z. Ye, F. Zhuge, Y.J. Zeng, B.H. Zhao, L.P. Zhu, Appl. Phys. Lett. 85 (2004) 3134.
[8] A.V. Singh, R.M. Mehra, A. Wakahara, A. Yoshida, J. Appl. Phys. 93 (2003) 396.
[9] M. Joseph, H. Tabata, H. Saeki, K. Ueda, T. Kawai, Physica B 302–303 (2001) 140.
[10] L.G. Wang, A. Zunger, Phys. Rev. Lett. 90 (2003) 256401.
[11] S. Limpijumnong, S.B. Zhang, S.-H. Wei, C.H. Park, Phys. Rev. Lett. 92 (2004) 155504.
[12] X.-Y. Li, H.-J. Li, Z.-J. Wang, H. Xia, Z.-Y. Xiong, J.-X. Wang, B.-C. Yang, Opt. Commun. 282 (2009) 247.
[13] Q.H. Li, D. Zhu, W. Liu, Y. Liu, X.C. Ma, Appl. Surf. Sci. 254 (2008) 2922.
[14] K.S. Huh, D.K. Hwang, K.H. Bang, M.K. Hong, D.H. Lee, J.M. Myong, M.S. Oh, K. Choi, Mater. Res. Soc. Symp. Proc. 692 (2002) 649.
[15] J. Wang, V. Sallet, F. Jomard, A.M.B. do Rego, E. Elamurugu, R. Martins, E. Fortunato, Thin Solid Films 515 (2007) 8780.
[16] J.C. Fan, Z. Xie, Mater. Sci. Eng. B 150 (2008) 61.
[17] T. Li-dan, W. Bing, Z. Yue, J. Alloys Compd. 509 (2011) 384.
[18] A. Kumar, M. Kumar, B.P. Singh, Appl. Surf. Sci. 256 (2010) 7200.
[19] J. Su, C. Zang, C. Cheng, Q. Niu, Y. Zhang, K. Yu, Appl. Surf. Sci. 257 (2010) 160.
[20] S.L. King, J.G.E. Gardeniers, I.W. Boyd, Appl. Surf. Sci. 9698 (1996) 811.
[21] M. Ding, B. Yao, D. Zhao, F. Fang, D. Shen, Z. Zhang, Thin Solid Films 518 (2010) 4390.
[22] S. Limpijumnong, M.F. Smith, S.B. Zhang, Appl. Phys. Lett. 89 (2006) 222113.
[23] K.P. Bhuvana, J. Elanchezhiyan, N. Gopalakrishnan, T. Balasubramanian, Appl. Surf. Sci. 255 (2008) 2026.
[24] N. Xu, Y. Xu, L. Li, Y. Shen, T. Zhang, J. Wu, J. Sun, Z. Ying, J. Vac. Sci. Technol. A 24 (2006) 517.
[25] J.C. Sun, J.Z. Zhao, H.W. Liang, J.M. Bian, L.Z. Hu, H.Q. Zhang, X.P. Liang, W.F. Liu, G.T. Du, Appl. Phys. Lett. 90 (2007) 121128.
[26] G. Du, Y. Cui, X. Xiaochuan, X. Li, H. Zhu, B. Zhang, Y. Zhang, Y. Ma, Appl. Phys. Lett. 90 (2007) 243504.
[27] T. Yamamoto, H.K. Yoshida, Physica B 302–303 (2001) 155.
[28] X.M. Duan, C. Stampfl, M.M.M. Bilek, D.R. McKenzie, Phys. Rev. B 79 (2009) 235208.
[29] Y.R. Ryu, T.S. Lee, J.A. Lubguban, H.W. White, Y.S. Park, C.J. Youn, Appl. Phys. Lett. 87 (2005) 153504.
[30] K. Vanheusden, W.L. Warren, C.H. Seager, D.R. Tallant, J.A. Voigt, B.E. Gnade, J. Appl. Phys. 79 (1996) 7983.
[31] D.H. Fan, Z.Y. Ning, M.F. Jiang, Appl. Surf. Sci. 245 (2005) 414.
[32] Y.J. Lin, C.L. Tsai, Y.M. Lu, C.J. Liu, J. Appl. Phys. 99 (2006) 093501.
[33] Y.R. Ryu, T.S. Lee, H.W. White, Appl. Phys. Lett. 83 (2003) 87.
[34] F.X. Xiu, Z. Yang, L.J. Mandalapu, D.T. Zhao, J.L. Liua, Appl. Phys. Lett. 87 (2005) 252102.
[35] Y. Ma, G.T. Du, S.R. Yang, Z.T. Li, B.J. Zhao, X.T. Yang, T.P. Yang, Y.T. Zhang, D.L. Liu, J. Appl. Phys. 95 (2004) 6268.
[36] D.J. Rogers, F. Hosseini Teherani, T. Monteiro, M. Soares, A. Neves, et al., Phys. Status Solidi C 3 (2006) 1038.
[37] H. Tang, Z. Ye, H. He, Opt. Mater. 30 (2008) 1422.

[38] D.C. Look, D.C. Reynolds, C.W. Litton, R.L. Jones, D.B. Eason, G. Cantwell, Appl. Phys. Lett. 81 (10) (2002) 1830.
[39] H.S. Kang, G.H. Kim, D.L. Kim, H.W. Chang, B.D. Ahn, S.Y. Lee, Appl. Phys. Lett. 89 (2006) 181103.
[40] S.S. Lin, J.G. Lu, Z.Z. Ye, H.P. He, X.Q. Gu, L.X. Chen, J.Y. Huang, B.H. Zhao, Solid State Commun. 148 (2008) 25.
[41] J.C. Fan, C.Y. Zhu, S. Fung, Y.C. Zhong, K.S. Wong, Z. Xie, G. Brauer, W. Anwand, W. Skorupa, C.K. To, B. Yang, C.D. Beling, C.C. Ling, J. Appl. Phys. 106 (2009) 073709.
[42] Y.H. Tak, K.B. Kim, H.G. Park, K.H. Lee, J.R. Lee, Thin Solid Films 411 (2002) 12.